mathematics

MDPI

Article

Stability and Local Bifurcations of a Discrete Predator–Prey System with Allee Effect and Holling-IV Functional Response

Jingwen Chen and Xianyi Li *

Department of Big Data Science, School of Science, Zhejiang University of Science and Technology, Hangzhou 310023, China
* Correspondence: mathxyli@zust.edu.cn

Abstract

This paper investigates the local dynamics of a discrete predator–prey system incorporating an Allee effect and a Holling-IV functional response. After nondimensionalization, a positivity-preserving discrete model is obtained by the semi-discretization method. The non-negative fixed points are classified and their local stability is established. The center manifold theorem and local bifurcation theory are then used to prove two transcritical bifurcations at the boundary fixed points E_1 and E_2 and a saddle-node bifurcation at the positive critical fixed point E^*. Numerical equilibrium branch diagrams and phase portraits illustrate these local results. The possible Neimark–Sacker bifurcation at E_3 and flip bifurcation at E_4 are beyond the present scope of this study.

Keywords: discrete predator–prey system; Allee effect; Holling-IV functional response; semi-discretization method; transcritical bifurcation; saddle-node bifurcation; Neimark–Sacker bifurcation.

MSC: 39A28; 39A30

Check for updates

Academic Editor: Davide Valenti

Received: 22 July 2026
Revised: 31 August 2026
Accepted: 2 September 2026
Published: 4 September 2026

1. Introduction and Preliminaries

Predator–prey models provide a basic framework for studying coexistence, extinction, stability, oscillations, and bifurcations [1,2]. Classical models often assume logistic prey growth, whereas a population at low density may exhibit reduced per capita growth or decline because of a strong Allee effect [2–5]. This mechanism may alter the number and stability of biologically meaningful equilibria and create threshold-dependent outcomes.

Holling type-I models may exhibit limit cycles, Hopf and cyclic-fold bifurcations, and bistability [3,6]; Holling type-II saturation may cause stability loss, Hopf bifurcations, and multiple limit cycles [1,7]; and Holling type-III responses can produce stability changes, Bogdanov–Takens, flip, and Neimark–Sacker bifurcations, and chaos [4,5,8,9]. Unlike these monotone responses, the simplified Holling-IV response is nonmonotone and represents inhibition at high prey density [10,11]. The closest studies differ from the present paper. References [12,13] investigate discrete predator–prey models with nonmonotone functional responses and derive stability and bifurcation results. Reference [11] also uses semi-discretization, but for a Leslie-type, ratio-dependent model with logistic prey growth, and analyzes one positive fixed point together with flip and Neimark–Sacker bifurcations. Reference [14] combines an Allee effect with Holling type-I predation and shows that changing the discretization can remove a reported flip bifurcation while yielding Neimark–Sacker and transcritical conditions. In contrast, the present map couples a strong Allee threshold with inhibitory Holling-IV predation, classifies zero, one, or two positive fixed points, and proves a saddle-node bifurcation at the collision of the two positive branches. Thus, the contribution lies in this interaction and the resulting equilibrium multiplicity, rather than in the standard boundary transcritical calculations alone.

Accordingly, the corresponding continuous predator–prey model takes the form [11]

$$\begin{cases} \dfrac{dx}{dt} = rx\Big(1 - \dfrac{x}{K}\Big)(x - m) - \dfrac{px}{x^2 + a}y, \\ \dfrac{dy}{dt} = \dfrac{epx}{x^2 + a}y - dy. \end{cases} \tag{1}$$

A strong Allee effect is characterized by a negative per capita growth rate below a positive population threshold and a positive rate immediately above it. In the absence of predators ($y = 0$), the prey per capita growth rate is $G(x) = r(1 - x/K)(x - m)$. Since $0 < m < K$, $G(x) < 0$ for $0 < x < m$ and $G(x) > 0$ for $m < x < K$. Thus, m is a positive strong Allee threshold. The variables and parameters are listed in Table 1.

Table 1. Biological meanings of variables and parameters in system (1).

Symbol	Biological Meaning
$x(t)$	Density of the prey population at time t
$y(t)$	Density of the predator population at time t
r	Growth coefficient of the prey (density-dependent)
K	Environmental carrying capacity of the prey
m	Allee threshold of the prey population
p	Scaling parameter of the predation rate
a	Inhibition parameter of the functional response
e	Conversion efficiency of the predator
d	Death rate of the predator

For the simplified Holling-IV functional response

$$H(x) = \frac{px}{x^2 + a},$$

direct differentiation gives

$$H'(x) = \frac{p(a - x^2)}{(x^2 + a)^2}.$$

Hence, $H(x)$ increases for $0 < x < \sqrt{a}$, decreases for $x > \sqrt{a}$, and attains its maximum

$$H(\sqrt{a}) = \frac{p}{2\sqrt{a}}$$

at $x = \sqrt{a}$. Thus, p linearly scales the overall magnitude of the predation response without changing the location of its maximum, whereas a determines the prey-density level at which the response changes from increasing to decreasing and also influences the maximum response value. Since a is added to x^2, it has the dimensions of prey density squared and is not a conventional half-saturation constant. The decreasing response for $x > \sqrt{a}$ represents inhibition of predation at sufficiently high prey density, which is the ecological mechanism described by the simplified Holling-IV form.

For mathematical convenience, we first nondimensionalize system (1). Let

$$u = \frac{x}{K}, \qquad v = \frac{p}{rK^3}y, \qquad \tau = rKt.$$

https://doi.org/10.3390/math14173198

Furthermore, define the dimensionless parameters

$$\mu = \frac{m}{K}, \qquad \alpha = \frac{a}{K^2}, \qquad \beta = \frac{ep}{rK^2}, \qquad \gamma = \frac{d}{rK}.$$

Since $0 < m < K$, we have $0 < \mu < 1$.

Substituting these transformations into system (1), we derive the following nondimensional system:

$$\begin{cases} \dfrac{du}{d\tau} = u(1-u)(u-\mu) - \dfrac{uv}{u^2+\alpha}, \\ \dfrac{dv}{d\tau} = v\left(\dfrac{\beta u}{u^2+\alpha} - \gamma\right), \end{cases} \tag{2}$$

where

$$0 < \mu < 1, \qquad \alpha > 0, \qquad \beta > 0, \qquad \gamma > 0.$$

In many ecological systems, population densities are observed at discrete time intervals. Moreover, discrete models may exhibit richer dynamics than their continuous counterparts, such as bifurcation, periodic oscillation, and chaos [9,12,13]. Therefore, it is natural to study the discrete version of system (2).

Now, we use a semi-discretization method to discretize system (2). Let $[\tau]$ denote the greatest integer not exceeding τ. Consider the average rates of change of system (2) at integer times, namely, the following model [14]:

$$\begin{cases} \dfrac{1}{u(\tau)}\dfrac{du}{d\tau} = (1-u([\tau]))(u([\tau])-\mu) - \dfrac{v([\tau])}{u^2([\tau])+\alpha}, \\ \dfrac{1}{v(\tau)}\dfrac{dv}{d\tau} = \dfrac{\beta u([\tau])}{u^2([\tau])+\alpha} - \gamma. \end{cases} \tag{3}$$

One can see that a solution $(u(\tau), v(\tau))$ of system (3) for $\tau \in [0, +\infty)$ has the following properties:

1. On the interval $[0, +\infty)$, $u(\tau)$ and $v(\tau)$ are continuous.
2. $\dfrac{du}{d\tau}$ and $\dfrac{dv}{d\tau}$ exist everywhere when $\tau \in [0, +\infty)$, except possibly at the points $\{0, 1, 2, \ldots\}$.
3. System (3) holds on any interval $[n, n+1)$ with $n = 0, 1, 2, \ldots$.

The following system can be obtained by integrating system (3) over the interval $[n, \tau]$ for any $\tau \in [n, n+1)$ and $n = 0, 1, 2, \ldots$:

$$\begin{cases} \ln \dfrac{u(\tau)}{u(n)} = \left[(1-u_n)(u_n-\mu) - \dfrac{v_n}{u_n^2+\alpha}\right](\tau - n), \\ \ln \dfrac{v(\tau)}{v(n)} = \left[\dfrac{\beta u_n}{u_n^2+\alpha} - \gamma\right](\tau - n). \end{cases} \tag{4}$$

where $u_n = u(n)$ and $v_n = v(n)$.

Exponentiating both equations in system (4), we obtain

$$\begin{cases} u(\tau) = u_n \exp\left\{\left[(1-u_n)(u_n-\mu) - \dfrac{v_n}{u_n^2+\alpha}\right](\tau - n)\right\}, \\ v(\tau) = v_n \exp\left\{\left[\dfrac{\beta u_n}{u_n^2+\alpha} - \gamma\right](\tau - n)\right\}. \end{cases} \tag{5}$$

Letting $\tau \to (n+1)^-$ in system (5) produces

$$\begin{cases} u_{n+1} = u_n \exp\left[(1-u_n)(u_n-\mu) - \dfrac{v_n}{u_n^2+\alpha}\right], \\ v_{n+1} = v_n \exp\left[\dfrac{\beta u_n}{u_n^2+\alpha} - \gamma\right]. \end{cases} \tag{6}$$

where

$$0 < \mu < 1, \qquad \alpha > 0, \qquad \beta > 0, \qquad \gamma > 0.$$

and the parameters are the same as in system (2). System (6) will be considered in the sequel. It is easy to see that if $u_0 > 0$ and $v_0 > 0$, then $u_n > 0$ and $v_n > 0$ for all $n \geq 0$. Hence, the positive quadrant is positively invariant under system (6), which is consistent with the biological meaning of prey and predator populations.

Scope Limitation. The positivity argument above establishes only forward invariance of the positive quadrant; it does not prove boundedness, dissipativity, the existence of a compact absorbing region, uniform persistence, or a global basin structure. Accordingly, all stability and bifurcation conclusions below are local and do not imply global predator persistence or coexistence for arbitrary initial conditions. Sections 2–5 present the fixed-point analysis, local bifurcations, numerical illustrations, and conclusions.

In the semi-discretization above, unit intervals $[n, n+1)$ are used in the dimensionless time τ, so system (6) has the fixed step $h = 1$. Since $\tau = rKt$, one iteration corresponds to $\dfrac{1}{rK}$ units of the original time. This is a modeling convention rather than a consequence forced by nondimensionalization. For a general $h > 0$, both exponents in (6) would be multiplied by h. The fixed points and the critical values β_0, β_1, and β_2 remain unchanged, whereas the Jacobian multipliers and stability may depend on h. Therefore, all results in this paper concern $h = 1$; a systematic analysis for general h is left for future work.

2. Existence and Stability of Fixed Points

2.1. Existence of Fixed Points

In this subsection, we discuss the existence of non-negative fixed points of the discrete system (6).

Let $E = (u, v)$ be a fixed point of system (6). Then, its coordinates satisfy

$$\begin{cases} u = u \exp\left[(1-u)(u-\mu) - \dfrac{v}{u^2+\alpha}\right], \\ v = v \exp\left[\dfrac{\beta u}{u^2+\alpha} - \gamma\right]. \end{cases} \tag{7}$$

It is easy to see that system (6) always has the following three boundary fixed points:

$$E_0 = (0, 0), \qquad E_1 = (1, 0), \qquad E_2 = (\mu, 0).$$

We now consider positive fixed points. Suppose that $u > 0$ and $v > 0$. Then, from (7), we have

$$(1-u)(u-\mu) - \frac{v}{u^2+\alpha} = 0, \tag{8}$$

and

$$\frac{\beta u}{u^2+\alpha} - \gamma = 0. \tag{9}$$

By (8), we obtain

$$v = (u^2+\alpha)(1-u)(u-\mu). \tag{10}$$

Since $v > 0$, it follows directly from (10) that

$$\mu < u < 1. \tag{11}$$

Equation (9) is equivalent to

$$\beta = \gamma \frac{u^2 + \alpha}{u} = \gamma\left(u + \frac{\alpha}{u}\right). \tag{12}$$

Therefore, the existence of positive fixed points is equivalent to the existence of roots of

$$\phi(u) = \gamma\left(u + \frac{\alpha}{u}\right) - \beta = 0 \tag{13}$$

in the interval $(\mu, 1)$.

For later use, define

$$\beta_0 := 2\gamma\sqrt{\alpha}, \qquad \beta_1 := \gamma(1+\alpha), \qquad \beta_2 := \gamma\frac{\mu^2 + \alpha}{\mu}. \tag{14}$$

By direct calculation,

$$\phi'(u) = \gamma\left(1 - \frac{\alpha}{u^2}\right).$$

By the arithmetic-geometric mean inequality,

$$\beta_1 = \gamma(1+\alpha) \geq 2\gamma\sqrt{\alpha} = \beta_0, \qquad \beta_2 = \gamma\left(\mu + \frac{\alpha}{\mu}\right) \geq 2\gamma\sqrt{\alpha} = \beta_0,$$

where equality holds if and only if $\alpha = 1$ and $\alpha = \mu^2$, respectively. Moreover,

$$\beta_1 - \beta_2 = \frac{\gamma(1-\mu)(\mu-\alpha)}{\mu}.$$

Since $\gamma > 0$ and $0 < \mu < 1$, it follows that $\beta_1 > \beta_2$, $\beta_1 = \beta_2$, or $\beta_1 < \beta_2$ according as $\alpha < \mu$, $\alpha = \mu$, or $\alpha > \mu$. Combining these comparisons gives all the orderings used in Table 2.

Finally, $\phi(\mu) = \beta_2 - \beta$, $\phi(1) = \beta_1 - \beta$, and, when $\mu < \sqrt{\alpha} < 1$, $\phi(\sqrt{\alpha}) = \beta_0 - \beta$. Since ϕ' changes sign only at $\sqrt{\alpha}$, ϕ is increasing on $(\mu, 1)$ for $\alpha \leq \mu^2$, decreasing there for $\alpha \geq 1$, and decreases and then increases for $\mu^2 < \alpha < 1$. Comparing these values with zero yields exactly the classification in Table 2.

Here, throughout the table,

$$u_1 = \frac{\beta - \sqrt{\beta^2 - 4\gamma^2\alpha}}{2\gamma}, \qquad u_2 = \frac{\beta + \sqrt{\beta^2 - 4\gamma^2\alpha}}{2\gamma},$$

and

$$v_i = (u_i^2 + \alpha)(1 - u_i)(u_i - \mu), \qquad i = 1, 2. \tag{15}$$

When two positive fixed points exist,

$$E_3 = (u_1, v_1), \qquad E_4 = (u_2, v_2),$$

and, in particular,

$$\mu < u_1 < \sqrt{\alpha} < u_2 < 1.$$

Table 2. Classification of positive fixed points.

Range of α	Range of β	Number	Positive Fixed Point (s)
$0 < \alpha \leq \mu^2$	$\beta_2 < \beta < \beta_1$	1	$E_4 = (u_2, v_2)$
$\mu^2 < \alpha < \mu$	$\beta = \beta_0$	1	$E^* = (\sqrt{\alpha}, 2\alpha(1-\sqrt{\alpha})(\sqrt{\alpha}-\mu))$
	$\beta_0 < \beta < \beta_2$	2	$E_3 = (u_1, v_1), \quad E_4 = (u_2, v_2)$
	$\beta_2 \leq \beta < \beta_1$	1	$E_4 = (u_2, v_2)$
$\alpha = \mu$	$\beta = \beta_0$	1	$E^* = (\sqrt{\alpha}, 2\alpha(1-\sqrt{\alpha})(\sqrt{\alpha}-\mu))$
	$\beta_0 < \beta < \beta_1$	2	$E_3 = (u_1, v_1), \quad E_4 = (u_2, v_2)$
$\mu < \alpha < 1$	$\beta = \beta_0$	1	$E^* = (\sqrt{\alpha}, 2\alpha(1-\sqrt{\alpha})(\sqrt{\alpha}-\mu))$
	$\beta_0 < \beta < \beta_1$	2	$E_3 = (u_1, v_1), \quad E_4 = (u_2, v_2)$
	$\beta_1 \leq \beta < \beta_2$	1	$E_3 = (u_1, v_1)$
$\alpha \geq 1$	$\beta_1 < \beta < \beta_2$	1	$E_3 = (u_1, v_1)$
In all other parameter regions, system (6) has no positive fixed point.			

2.2. Local Stability of Fixed Points

Before analyzing the local stability of fixed points, we first introduce the following definition and lemma.

Definition 1. *Let $E(x, y)$ be a fixed point of a two-dimensional discrete system with multipliers λ_1 and λ_2:*

(i) *If $|\lambda_1| < 1$ and $|\lambda_2| < 1$, then $E(x, y)$ is called a sink, and a sink is locally asymptotically stable.*
(ii) *If $|\lambda_1| > 1$ and $|\lambda_2| > 1$, then $E(x, y)$ is called a source, and a source is locally asymptotically unstable.*
(iii) *If $|\lambda_1| < 1$ and $|\lambda_2| > 1$, or $|\lambda_1| > 1$ and $|\lambda_2| < 1$, then $E(x, y)$ is called a saddle.*
(iv) *If either $|\lambda_1| = 1$ or $|\lambda_2| = 1$, then $E(x, y)$ is called non-hyperbolic.*

Lemma 1. *Let*

$$F(\lambda) = \lambda^2 + B\lambda + C,$$

where B and C are two real constants. Suppose that λ_1 and λ_2 are two roots of $F(\lambda) = 0$. Then, the following statements hold:

(i) *If $F(1) > 0$, then*
  (i.1) *$|\lambda_1| < 1$ and $|\lambda_2| < 1$ if and only if $F(-1) > 0$ and $C < 1$;*
  (i.2) *$\lambda_1 = -1$ and $\lambda_2 \neq -1$ if and only if $F(-1) = 0$ and $B \neq 2$;*
  (i.3) *$|\lambda_1| < 1$ and $|\lambda_2| > 1$ if and only if $F(-1) < 0$;*
  (i.4) *$|\lambda_1| > 1$ and $|\lambda_2| > 1$ if and only if $F(-1) > 0$ and $C > 1$;*
  (i.5) *λ_1 and λ_2 are a pair of conjugate complex roots and $|\lambda_1| = |\lambda_2| = 1$ if and only if $-2 < B < 2$ and $C = 1$;*
  (i.6) *$\lambda_1 = \lambda_2 = -1$ if and only if $F(-1) = 0$ and $B = 2$.*
(ii) *If $F(1) = 0$, namely, 1 is one root of $F(\lambda) = 0$, then the other root λ satisfies $|\lambda| < (=, >)1$ according to $|C| < (=, >)1$.*
(iii) *If $F(1) < 0$, then $F(\lambda) = 0$ has one root lying in $(1, +\infty)$. Moreover, we have the following:*
  (iii.1) *The other root λ satisfies $\lambda < -1$ if and only if $F(-1) < 0$ and satisfies $\lambda = -1$ if and only if $F(-1) = 0$;*
  (iii.2) *The other root satisfies $-1 < \lambda < 1$ if and only if $F(-1) > 0$.*

A direct calculation for system (6) gives

$$J(u,v) = \begin{pmatrix} \left[1 + u(1 + \mu - 2u) + \dfrac{2u^2 v}{(u^2+\alpha)^2}\right] e^{(1-u)(u-\mu) - \frac{v}{u^2+\alpha}} & -\dfrac{u}{u^2+\alpha} e^{(1-u)(u-\mu) - \frac{v}{u^2+\alpha}} \\ \beta v \dfrac{\alpha - u^2}{(u^2+\alpha)^2} e^{\frac{\beta u}{u^2+\alpha} - \gamma} & e^{\frac{\beta u}{u^2+\alpha} - \gamma} \end{pmatrix}.$$

2.2.1. Local Stability of Boundary Fixed Points

At $E_0 = (0,0)$, the Jacobian matrix is

$$J(E_0) = \begin{pmatrix} e^{-\mu} & 0 \\ 0 & e^{-\gamma} \end{pmatrix}.$$

Since $0 < e^{-\mu} < 1$ and $0 < e^{-\gamma} < 1$, E_0 is a sink and hence is locally asymptotically stable. In what follows, we analyze the local stability of the two nonzero boundary fixed points

$$E_1 = (1,0), \qquad E_2 = (\mu,0).$$

By applying Definition 1 to the eigenvalues of the Jacobian matrix, we obtain the following local stability results for the boundary fixed points $E_1 = (1,0)$ and $E_2 = (\mu,0)$, respectively.

Theorem 1. *For the boundary fixed point $E_1 = (1,0)$ of system (6), the following statements are true:*

(1) If $0 < \beta < \beta_1$, then E_1 is a sink;
(2) If $\beta = \beta_1$, then E_1 is non-hyperbolic;
(3) If $\beta > \beta_1$, then E_1 is a saddle.

Proof. At $E_1 = (1,0)$, the Jacobian matrix is

$$J(E_1) = \begin{pmatrix} \mu & -\dfrac{1}{1+\alpha} \\ 0 & \exp\left(\dfrac{\beta}{1+\alpha} - \gamma\right) \end{pmatrix}.$$

Since $J(E_1)$ is an upper triangular matrix, its eigenvalues are

$$\lambda_1 = \mu, \qquad \lambda_2 = \exp\left(\frac{\beta}{1+\alpha} - \gamma\right).$$

Since $0 < \mu < 1$, $|\lambda_1| < 1$. Hence the local stability of E_1 is determined by λ_2. Moreover, since $\lambda_2 > 0$, one has $\lambda_2 < 1$, $\lambda_2 = 1$, or $\lambda_2 > 1$ when $\beta < \beta_1$, $\beta = \beta_1$, or $\beta > \beta_1$, respectively. □

Remark 1. *Theorem 1 describes the ecological state where the prey population persists at its carrying capacity while the predator is absent, corresponding to $E_1 = (1,0)$. When β is small, the energy gain from predation is insufficient to sustain predator growth, and a predator population introduced at sufficiently low density eventually dies out, leading the system to remain in a prey-only state. When β exceeds the critical value β_1, this state loses stability, indicating that predators are able to invade and alter the ecosystem structure.*

Theorem 2. *The local stability of the boundary fixed point $E_2 = (\mu,0)$ of system (6) is classified as follows:*

(1) *If* $0 < \beta < \beta_2$*, then* E_2 *is a saddle;*
(2) *If* $\beta = \beta_2$*, then* E_2 *is non-hyperbolic;*
(3) *If* $\beta > \beta_2$*, then* E_2 *is a source.*

Proof. At $E_2 = (\mu, 0)$, the Jacobian matrix is

$$J(E_2) = \begin{pmatrix} 1 + \mu - \mu^2 & -\dfrac{\mu}{\mu^2 + \alpha} \\ 0 & \exp\left(\dfrac{\beta\mu}{\mu^2 + \alpha} - \gamma\right) \end{pmatrix}.$$

Since $J(E_2)$ is an upper triangular matrix, its eigenvalues are

$$\lambda_1 = 1 + \mu - \mu^2, \qquad \lambda_2 = \exp\left(\frac{\beta\mu}{\mu^2 + \alpha} - \gamma\right).$$

Since $0 < \mu < 1$, we have

$$\lambda_1 = 1 + \mu - \mu^2 = 1 + \mu(1 - \mu) > 1.$$

Thus,

$$|\lambda_1| > 1.$$

Since $\lambda_2 > 0$, we have $\lambda_2 < 1$, $\lambda_2 = 1$, or $\lambda_2 > 1$ when $\beta < \beta_2$, $\beta = \beta_2$, or $\beta > \beta_2$, respectively. □

From the above theorems, the boundary fixed point E_1 changes from a sink to a saddle as β passes through the critical value β_1, while E_2 changes from a saddle to a source as β passes through the critical value β_2. In both critical cases, the Jacobian matrix has an eigenvalue $\lambda = 1$, which will be considered in the subsequent bifurcation analysis.

Remark 2. *Theorem 2 corresponds to the state* $E_2 = (\mu, 0)$*, where the prey population is at the Allee threshold and the predator is absent. This state represents a critical low-density survival boundary for the prey population under the Allee effect. The result shows that this equilibrium is not robust to perturbations or predation pressure, and the system tends to move away from this threshold state, leading to alternative population dynamics.*

2.2.2. Local Stability of Positive Fixed Points

In this subsubsection, we discuss the local stability of positive fixed points of system (6). Let $E = (u, v)$ be a positive fixed point of system (6). Then,

$$\mu < u < 1,$$

and

$$v = (u^2 + \alpha)(1 - u)(u - \mu),$$
$$\frac{\beta u}{u^2 + \alpha} = \gamma.$$

At a positive fixed point, the two exponential terms in the Jacobian matrix are equal to 1. Thus, the Jacobian matrix at $E = (u, v)$ becomes

$$J(E) = \begin{pmatrix} 1 + u(1 + \mu - 2u) + \dfrac{2u^2(1 - u)(u - \mu)}{u^2 + \alpha} & -\dfrac{u}{u^2 + \alpha} \\ \dfrac{\beta v(\alpha - u^2)}{(u^2 + \alpha)^2} & 1 \end{pmatrix},$$

The characteristic equation of $J(E)$ can be written as

$$F(\lambda) = \lambda^2 + B(u)\lambda + C(u),$$

where

$$B(u) = -\left[2 + u(1+\mu-2u) + \frac{2u^2(1-u)(u-\mu)}{u^2+\alpha}\right],$$

and

$$C(u) = 1 + u(1+\mu-2u) + \frac{2u^2(1-u)(u-\mu)}{u^2+\alpha} + \gamma\frac{(1-u)(u-\mu)(\alpha-u^2)}{u^2+\alpha}.$$

Therefore,

$$F(1) = \gamma\frac{(1-u)(u-\mu)(\alpha-u^2)}{u^2+\alpha},$$

and

$$F(-1) = 4 + 2u(1+\mu-2u) + \frac{4u^2(1-u)(u-\mu)}{u^2+\alpha} + \gamma\frac{(1-u)(u-\mu)(\alpha-u^2)}{u^2+\alpha}.$$

Based on the characteristic equation obtained above and in Lemma 1, we now summarize the local stability of the positive fixed points.

For convenience, define

$$\delta = \frac{[4+2u_2(1+\mu-2u_2)](u_2^2+\alpha) + 4u_2^2(1-u_2)(u_2-\mu)}{(1-u_2)(u_2-\mu)(u_2^2-\alpha)},$$

$$\Gamma_{u_1} = u_1(1+\mu-2u_1) + \frac{2u_1^2(1-u_1)(u_1-\mu)}{u_1^2+\alpha} + \gamma\frac{(1-u_1)(u_1-\mu)(\alpha-u_1^2)}{u_1^2+\alpha}.$$

Here δ is an equilibrium-dependent threshold evaluated at $E_4 = (u_2, v_2)$. Since u_2 depends on the model parameters through (15), conditions expressed in terms of δ are implicit. For notational simplicity, we retain δ below; Γ_{u_1} is used for $E_3 = (u_1, v_1)$.

Then, the local stability of positive fixed points can be classified as follows. For any positive fixed point $E = (u, v)$, we have $\mu < u < 1$. Hence, from the expression of $F(1)$, the sign of $F(1)$ is determined by the sign of $\alpha - u^2$. Therefore, the stability of positive fixed points can be discussed according to the relative position of u and $\sqrt{\alpha}$.

First, consider the right-branch positive fixed point $E_4 = (u_2, v_2)$. Since $u_2 > \sqrt{\alpha}$, one has $F(1) < 0$. By Lemma 1, E_4 has an eigenvalue greater than 1. Its remaining stability is determined by the sign of $F(-1)$. Solving $F(-1) = 0$ gives the critical value δ. Therefore, E_4 is a saddle if $0 < \gamma < \delta$, non-hyperbolic if $\gamma = \delta$, and a source if $\gamma > \delta$.

Second, consider the critical positive fixed point E^*, where $u^* = \sqrt{\alpha}$. Here, $J(E^*)$ is upper triangular, and its two multipliers are

$$\lambda_1 = 1, \qquad \lambda_2 = \Lambda_* = 1 + 2\sqrt{\alpha} + 2\mu\sqrt{\alpha} - \mu - 3\alpha > 0.$$

Hence, E^* is non-hyperbolic.

Finally, for the left-branch positive fixed point $E_3 = (u_1, v_1)$, $\mu < u_1 < 1$ and $u_1 < \sqrt{\alpha}$; hence, $F(1) > 0$. Moreover,

$$F(-1) = 4(1-u_1^2) + 2u_1(1+\mu) + \frac{4u_1^2(1-u_1)(u_1-\mu)}{u_1^2+\alpha} + \gamma\frac{(1-u_1)(u_1-\mu)(\alpha-u_1^2)}{u_1^2+\alpha} > 0.$$

Every term is positive since $\gamma > 0$, $1 - u_1 > 0$, $u_1 - \mu > 0$, and $\alpha - u_1^2 > 0$. Thus, by Lemma 1, E_3 is a sink, non-hyperbolic, or a source according as $\Gamma_{u_1} < 0$, $\Gamma_{u_1} = 0$, or $\Gamma_{u_1} > 0$, respectively.

Combining the above three cases with the existence classification of positive fixed points in Section 2.1, we obtain the classifications summarized in Tables 3–5.

Table 3. Type of fixed point E^*.

Conditions		Eigenvalues	Properties
$\mu^2 < \alpha \leq \mu$	$\beta = \beta_0$	$\|\lambda_1\| = 1,\ \|\lambda_2\| > 1$	non-hyperbolic
$\mu < \alpha < 1$	$\beta = \beta_0$	$\|\lambda_1\| = 1,\ \|\lambda_2\| > 1$ or $\|\lambda_2\| < 1$	non-hyperbolic

Table 4. Type of fixed point E_3.

Conditions			Eigenvalues	Properties
$\mu^2 < \alpha < \mu$	$\beta_0 < \beta < \beta_2$		$\|\lambda_1\| > 1,\ \|\lambda_2\| > 1$	source
$\alpha = \mu$	$\beta_0 < \beta < \beta_1$		$\|\lambda_1\| > 1,\ \|\lambda_2\| > 1$	source
$\mu < \alpha < 1$	$\beta_0 < \beta < \beta_1$	$\Gamma_{u_1} > 0$	$\|\lambda_1\| > 1,\ \|\lambda_2\| > 1$	source
		$\Gamma_{u_1} = 0$	$\|\lambda_1\| = \|\lambda_2\| = 1$	non-hyperbolic
		$\Gamma_{u_1} < 0$	$\|\lambda_1\| < 1,\ \|\lambda_2\| < 1$	sink
$\alpha \geq 1$	$\beta_1 < \beta < \beta_2$	$\Gamma_{u_1} > 0$	$\|\lambda_1\| > 1,\ \|\lambda_2\| > 1$	source
		$\Gamma_{u_1} = 0$	$\|\lambda_1\| = \|\lambda_2\| = 1$	non-hyperbolic
		$\Gamma_{u_1} < 0$	$\|\lambda_1\| < 1,\ \|\lambda_2\| < 1$	sink

Table 5. Type of fixed point E_4.

Conditions			Eigenvalues	Properties
$0 < \alpha \leq \mu^2$	$\beta_2 < \beta < \beta_1$	$0 < \gamma < \delta$	$\|\lambda_1\| > 1,\ \|\lambda_2\| < 1$	saddle
		$\gamma = \delta$	$\|\lambda_1\| > 1,\ \|\lambda_2\| = 1$	non-hyperbolic
		$\gamma > \delta$	$\|\lambda_1\| > 1,\ \|\lambda_2\| > 1$	source
$\mu^2 < \alpha < \mu$	$\beta_0 < \beta < \beta_1$	$0 < \gamma < \delta$	$\|\lambda_1\| > 1,\ \|\lambda_2\| < 1$	saddle
		$\gamma = \delta$	$\|\lambda_1\| > 1,\ \|\lambda_2\| = 1$	non-hyperbolic
		$\gamma > \delta$	$\|\lambda_1\| > 1,\ \|\lambda_2\| > 1$	source
$\alpha = \mu$	$\beta_0 < \beta < \beta_1$	$0 < \gamma < \delta$	$\|\lambda_1\| > 1,\ \|\lambda_2\| < 1$	saddle
		$\gamma = \delta$	$\|\lambda_1\| > 1,\ \|\lambda_2\| = 1$	non-hyperbolic
		$\gamma > \delta$	$\|\lambda_1\| > 1,\ \|\lambda_2\| > 1$	source
$\mu < \alpha < 1$	$\beta_0 < \beta < \beta_1$	$0 < \gamma < \delta$	$\|\lambda_1\| > 1,\ \|\lambda_2\| < 1$	saddle
		$\gamma = \delta$	$\|\lambda_1\| > 1,\ \|\lambda_2\| = 1$	non-hyperbolic
		$\gamma > \delta$	$\|\lambda_1\| > 1,\ \|\lambda_2\| > 1$	source

3. Bifurcation Analysis

In this section, we employ the center manifold theorem and local bifurcation theory to establish the transcritical bifurcations at E_1 and E_2 and the saddle-node bifurcation at E^*. The potential Neimark–Sacker case at E_3 and flip case at E_4 can be studied within the same center-manifold and normal-form framework. However, their distinct higher-order transversality, nonresonance, and nondegeneracy calculations are substantially more involved; they are therefore omitted here and left for future work [15–18].

3.1. Main Results

From Theorem 1, $E_1 = (1, 0)$ is non-hyperbolic when $\beta = \beta_1$. Thus, a local bifurcation may occur near E_1 as β passes through the critical value β_1. The following result is obtained.

Theorem 3. *Assume that $\alpha \neq 1$. If β varies in a small neighborhood of β_1, then system (6) undergoes a transcritical bifurcation at $E_1 = (1, 0)$. Moreover, if $\alpha > 1$, the positive branch E_3 exists for $\beta > \beta_1$ and is locally asymptotically stable; if $0 < \alpha < 1$, the positive branch E_4 exists for $\beta < \beta_1$ and is a saddle.*

Remark 3. *Theorem 3 is a local result. Only when $\alpha > 1$ may nearby solutions approach the locally stable coexistence equilibrium. When $0 < \alpha < 1$, crossing β_1 does not imply successful predator establishment or stable coexistence.*

From Theorem 2, $E_2 = (\mu, 0)$ is non-hyperbolic when $\beta = \beta_2$. Similarly, a local bifurcation may occur near E_2 as β passes through the critical value β_2. We have the following result.

Theorem 4. *Assume that $\alpha \neq \mu^2$. System (6) undergoes a transcritical bifurcation at $E_2 = (\mu, 0)$ as β crosses β_2. Moreover, if $0 < \alpha < \mu^2$, the positive branch E_4 exists for $\beta > \beta_2$ and is a saddle; if $\alpha > \mu^2$, the positive branch E_3 exists for $\beta < \beta_2$ and is a source.*

Remark 4. *This result is also local. The point E_2 is a predator-free state with the prey exactly at the Allee threshold, not a prey-extinction state. Since the nearby positive branch is unstable in both cases, this bifurcation alone does not demonstrate predator persistence or stable coexistence.*

Remark 5. *The excluded cases $\alpha = 1$ in Theorem 3 and $\alpha = \mu^2$ in Theorem 4 are degenerate because the quadratic coefficient of the corresponding reduced map vanishes. Hence, the standard transcritical nondegeneracy condition fails, and higher-order terms or a higher-codimension unfolding must be considered. These cases are not investigated here.*

At the critical value $\beta = \beta_0$, the two positive fixed points coalesce at E^*. Hence, E^* is non-hyperbolic, and a local bifurcation may occur as β passes through β_0. We have the following result.

Theorem 5. *Assume that $\mu^2 < \alpha < 1$ and*

$$\alpha \neq \left(\frac{1 + \mu + \sqrt{\mu^2 - \mu + 1}}{3} \right)^2.$$

If the parameter β varies in a small neighborhood of β_0, then system (6) undergoes a saddle-node bifurcation at

$$E^* = \left(\sqrt{\alpha},\, 2\alpha(1 - \sqrt{\alpha})(\sqrt{\alpha} - \mu)\right).$$

Remark 6. *Theorem 5 shows that the two positive fixed points are created or annihilated when β crosses β_0. Thus, the saddle-node bifurcation produces an abrupt change in the number of locally available coexistence equilibria.*

3.2. Proofs of the Main Results

Proof of Theorem 3. From the stability analysis of boundary fixed points, the eigenvalues of the Jacobian matrix of system (6) at $E_1 = (1, 0)$ are

$$\lambda_1 = \mu, \qquad \lambda_2 = \exp\left(\frac{\beta}{1+\alpha} - \gamma\right).$$

Since $0 < \mu < 1$, one has

$$|\lambda_1| < 1.$$

When $\beta = \beta_1$, we have $\lambda_2 = 1$. Thus, E_1 is a non-hyperbolic fixed point and a bifurcation may occur at E_1.

To study the bifurcation at E_1, let $x_n = u_n - 1$ and $y_n = v_n$, and introduce a small perturbation parameter $\eta_n^* = \beta - \beta_1$ with $0 < |\eta_n^*| \ll 1$. Then, $u_n = 1 + x_n$, $v_n = y_n$, and $\beta = \beta_1 + \eta_n^*$. Furthermore, let $\eta_{n+1}^* = \eta_n^*$. Then, system (6) can be transformed into the following extended system:

$$\begin{cases} x_{n+1} = (1 + x_n)\exp\left[-x_n(1 - \mu + x_n) - \dfrac{y_n}{1 + \alpha + 2x_n + x_n^2}\right] - 1, \\ y_{n+1} = y_n \exp\left[(\beta_1 + \eta_n^*)\dfrac{1 + x_n}{1 + \alpha + 2x_n + x_n^2} - \gamma\right], \\ \eta_{n+1}^* = \eta_n^*. \end{cases} \tag{16}$$

Taking the Taylor expansion of system (16) at $(x_n, y_n, \eta_n^*) = (0, 0, 0)$, we obtain

$$\begin{cases} x_{n+1} = a_{100}x_n + a_{010}y_n + a_{200}x_n^2 + a_{110}x_n y_n + a_{020}y_n^2 + o(\rho_1^2), \\ y_{n+1} = b_{010}y_n + b_{110}x_n y_n + b_{011}y_n\eta_n^* + o(\rho_1^2), \\ \eta_{n+1}^* = \eta_n^*, \end{cases} \tag{17}$$

where $\rho_1 = \sqrt{x_n^2 + y_n^2 + (\eta_n^*)^2}$, and the coefficients are given by

$$\begin{aligned} &a_{100} = \mu, && a_{010} = -\frac{1}{1+\alpha}, && a_{200} = \frac{\mu^2 - 3}{2}, \\ &a_{110} = \frac{2}{(1+\alpha)^2} - \frac{\mu}{1+\alpha}, && a_{020} = \frac{1}{2(1+\alpha)^2}, && b_{010} = 1, \\ &b_{110} = \frac{\gamma(\alpha - 1)}{1+\alpha}, && b_{011} = \frac{1}{1+\alpha}. \end{aligned}$$

The linear part of system (17) is

$$\begin{pmatrix} x_{n+1} \\ y_{n+1} \\ \eta_{n+1}^* \end{pmatrix} = \begin{pmatrix} \mu & -\dfrac{1}{1+\alpha} & 0 \\ 0 & 1 & 0 \\ 0 & 0 & 1 \end{pmatrix} \begin{pmatrix} x_n \\ y_n \\ \eta_n^* \end{pmatrix}.$$

The eigenvalues of the above matrix are

$$\lambda_1 = \mu, \qquad \lambda_2 = 1, \qquad \lambda_3 = 1.$$

The corresponding eigenvectors can be chosen as

$$(1,0,0)^T, \qquad \left(\frac{1}{(1+\alpha)(\mu-1)},1,0\right)^T, \qquad (0,0,1)^T.$$

Thus, we take the transformation matrix

$$P=\begin{pmatrix}1 & \dfrac{1}{(1+\alpha)(\mu-1)} & 0\\ 0 & 1 & 0\\ 0 & 0 & 1\end{pmatrix}.$$

Let

$$\begin{pmatrix}x_n\\ y_n\\ \eta_n^*\end{pmatrix}=P\begin{pmatrix}X_n\\ Y_n\\ \eta_n\end{pmatrix}.$$

That is,

$$x_n=X_n+\frac{1}{(1+\alpha)(\mu-1)}Y_n, \qquad y_n=Y_n, \qquad \eta_n^*=\eta_n.$$

Under this transformation, system (17) becomes

$$\begin{cases}X_{n+1}=A_{100}X_n+A_{200}X_n^2+A_{110}X_nY_n+A_{020}Y_n^2+A_{011}Y_n\eta_n+o(\widetilde{\rho}_2^2),\\ Y_{n+1}=B_{010}Y_n+B_{110}X_nY_n+B_{020}Y_n^2+B_{011}Y_n\eta_n+o(\widetilde{\rho}_2^2),\\ \eta_{n+1}=\eta_n,\end{cases} \tag{18}$$

where $\widetilde{\rho}_2=\sqrt{X_n^2+Y_n^2+\eta_n^2}$, and the coefficients are

$$A_{100}=\mu, \qquad A_{200}=\frac{\mu^2-3}{2}, \qquad A_{110}=\frac{5+3\alpha-3\mu-\alpha\mu+\gamma(\alpha-1)}{(1+\alpha)^2(1-\mu)},$$

$$A_{020}=-\frac{\alpha\gamma+\alpha-\gamma-2\mu+3}{(1+\alpha)^3(1-\mu)^2}, \quad A_{011}=\frac{1}{(1+\alpha)^2(1-\mu)}, \quad B_{010}=1,$$

$$B_{110}=\frac{\gamma(\alpha-1)}{1+\alpha}, \qquad B_{020}=\frac{\gamma(1-\alpha)}{(1+\alpha)^2(1-\mu)}, \quad B_{011}=\frac{1}{1+\alpha}.$$

Now, we consider the center manifold. Let

$$X=h(Y,\eta),$$

where

$$h(0,0)=0, \qquad Dh(0,0)=0.$$

Assume that

$$h(Y,\eta)=c_{20}Y^2+c_{11}Y\eta+c_{02}\eta^2+o(\rho_2^2),$$

where $\rho_2=\sqrt{Y^2+\eta^2}$. Using the center manifold invariance equation

$$h(Y_{n+1},\eta_{n+1})=X_{n+1},$$

and comparing the coefficients of the second-order terms, we obtain

$$c_{20}=-\frac{\alpha\gamma+\alpha-\gamma-2\mu+3}{(1+\alpha)^3(1-\mu)^3}, \qquad c_{11}=\frac{1}{(1+\alpha)^2(1-\mu)^2}, \qquad c_{02}=0.$$

Therefore, the center manifold is given by

$$X = h(Y, \eta) = -\frac{\alpha\gamma + \alpha - \gamma - 2\mu + 3}{(1+\alpha)^3(1-\mu)^3} Y^2 + \frac{1}{(1+\alpha)^2(1-\mu)^2} Y\eta + o(\rho_2^2). \tag{19}$$

Restricting system (18) to the center manifold, we obtain the following reduced equation:

$$Y_{n+1} = g(Y_n, \eta_n),$$

where

$$g(Y, \eta) = Y + \frac{1}{1+\alpha} Y\eta + \frac{\gamma(1-\alpha)}{(1+\alpha)^2(1-\mu)} Y^2 + o(\rho_2^2). \tag{20}$$

From (20), we have

$$g(0,0) = 0, \qquad g_Y(0,0) = 1, \qquad g_\eta(0,0) = 0, \qquad g_{Y\eta}(0,0) = \frac{1}{1+\alpha} \neq 0.$$

Moreover,

$$g_{YY}(0,0) = \frac{2\gamma(1-\alpha)}{(1+\alpha)^2(1-\mu)}.$$

Since

$$\gamma > 0, \qquad 0 < \mu < 1,$$

we have

$$g_{YY}(0,0) \neq 0$$

if and only if

$$\alpha \neq 1.$$

Therefore, if $\alpha \neq 1$, then all the conditions for a transcritical bifurcation are satisfied. Hence, system (6) undergoes a transcritical bifurcation at $E_1 = (1,0)$ when $\beta = \beta_1$. This proves Theorem 3. □

Proof of Theorem 4. By the stability analysis of boundary fixed points, the eigenvalues of the Jacobian matrix of system (6) at $E_2 = (\mu, 0)$ are

$$\lambda_1 = 1 + \mu - \mu^2, \qquad \lambda_2 = \exp\left(\frac{\beta\mu}{\mu^2 + \alpha} - \gamma\right).$$

Because $0 < \mu < 1$, we have

$$\lambda_1 = 1 + \mu - \mu^2 = 1 + \mu(1-\mu) > 1.$$

At $\beta = \beta_2$, we have $\lambda_2 = 1$. Consequently, E_2 is a non-hyperbolic fixed point and a bifurcation may occur at E_2.

For the bifurcation analysis at E_2, let $x_n = u_n - \mu$ and $y_n = v_n$ and introduce a small perturbation parameter $\eta_n^* = \beta - \beta_2$ with $0 < |\eta_n^*| \ll 1$. Thus, $u_n = \mu + x_n$, $v_n = y_n$, and $\beta = \beta_2 + \eta_n^*$. In addition, let $\eta_{n+1}^* = \eta_n^*$. With these substitutions, system (6) can be transformed into the following extended system:

$$\begin{cases} x_{n+1} = (\mu + x_n)\exp\left[(1 - \mu - x_n)x_n - \dfrac{y_n}{\mu^2 + \alpha + 2\mu x_n + x_n^2}\right] - \mu, \\ y_{n+1} = y_n \exp\left[(\beta_2 + \eta_n^*)\dfrac{\mu + x_n}{\mu^2 + \alpha + 2\mu x_n + x_n^2} - \gamma\right], \\ \eta_{n+1}^* = \eta_n^*. \end{cases} \tag{21}$$

Expanding system (21) at $(x_n, y_n, \eta_n^*) = (0,0,0)$, we obtain

$$\begin{cases} x_{n+1} = \bar{a}_{100}x_n + \bar{a}_{010}y_n + \bar{a}_{200}x_n^2 + \bar{a}_{110}x_ny_n + \bar{a}_{020}y_n^2 + o(\rho_3^2), \\ y_{n+1} = \bar{b}_{010}y_n + \bar{b}_{110}x_ny_n + \bar{b}_{011}y_n\eta_n^* + o(\rho_3^2), \\ \eta_{n+1}^* = \eta_n^*, \end{cases} \tag{22}$$

where $\rho_3 = \sqrt{x_n^2 + y_n^2 + (\eta_n^*)^2}$, and the coefficients are

$$\bar{a}_{100} = 1 + \mu - \mu^2, \qquad \bar{a}_{010} = -\frac{\mu}{\mu^2 + \alpha}, \qquad \bar{a}_{200} = 1 - \frac{3}{2}\mu - \mu^2 + \frac{1}{2}\mu^3,$$

$$\bar{a}_{110} = \frac{2\mu^2}{(\mu^2 + \alpha)^2} - \frac{1 + \mu - \mu^2}{\mu^2 + \alpha}, \quad \bar{a}_{020} = \frac{\mu}{2(\mu^2 + \alpha)^2}, \quad \bar{b}_{010} = 1,$$

$$\bar{b}_{110} = \frac{\gamma(\alpha - \mu^2)}{\mu(\mu^2 + \alpha)}, \qquad \bar{b}_{011} = \frac{\mu}{\mu^2 + \alpha}.$$

The linear part of system (22) is

$$\begin{pmatrix} x_{n+1} \\ y_{n+1} \\ \eta_{n+1}^* \end{pmatrix} = \begin{pmatrix} 1 + \mu - \mu^2 & -\frac{\mu}{\mu^2 + \alpha} & 0 \\ 0 & 1 & 0 \\ 0 & 0 & 1 \end{pmatrix} \begin{pmatrix} x_n \\ y_n \\ \eta_n^* \end{pmatrix}.$$

The eigenvalues of the above matrix are

$$\lambda_1 = 1 + \mu - \mu^2, \qquad \lambda_2 = 1, \qquad \lambda_3 = 1.$$

The corresponding eigenvectors can be chosen as

$$(1, 0, 0)^T, \qquad \left(\frac{1}{(\mu^2 + \alpha)(1 - \mu)}, 1, 0 \right)^T, \qquad (0, 0, 1)^T.$$

Accordingly, we take the transformation matrix

$$P = \begin{pmatrix} 1 & \frac{1}{(\mu^2 + \alpha)(1 - \mu)} & 0 \\ 0 & 1 & 0 \\ 0 & 0 & 1 \end{pmatrix}.$$

Let

$$\begin{pmatrix} x_n \\ y_n \\ \eta_n^* \end{pmatrix} = P \begin{pmatrix} X_n \\ Y_n \\ \eta_n \end{pmatrix}.$$

Equivalently,

$$x_n = X_n + \frac{1}{(\mu^2 + \alpha)(1 - \mu)} Y_n, \qquad y_n = Y_n, \qquad \eta_n^* = \eta_n.$$

With this transformation, system (22) becomes

$$\begin{cases} X_{n+1} = \bar{A}_{100}X_n + \bar{A}_{200}X_n^2 + \bar{A}_{110}X_nY_n + \bar{A}_{020}Y_n^2 + \bar{A}_{011}Y_n\eta_n + o(\widetilde{\rho}_4^2), \\ Y_{n+1} = \bar{B}_{010}Y_n + \bar{B}_{110}X_nY_n + \bar{B}_{020}Y_n^2 + \bar{B}_{011}Y_n\eta_n + o(\widetilde{\rho}_4^2), \\ \eta_{n+1} = \eta_n, \end{cases} \tag{23}$$

where $\widetilde{\rho}_4 = \sqrt{X_n^2 + Y_n^2 + {\eta_n}^2}$, and the coefficients are

$$\bar{A}_{100} = 1 + \mu - \mu^2, \qquad \bar{A}_{200} = 1 - \frac{3}{2}\mu - \mu^2 + \frac{1}{2}\mu^3,$$

$$\bar{A}_{110} = \frac{\mu(\mu^2+\alpha)(1-3\mu) + 2\mu^3(1-\mu) - \gamma(\alpha-\mu^2)}{\mu(\mu^2+\alpha)^2(1-\mu)},$$

$$\bar{A}_{020} = -\frac{\alpha\gamma + \alpha\mu^2 - \gamma\mu^2 + 3\mu^4 - 2\mu^3}{\mu(\mu^2+\alpha)^3(1-\mu)^2}, \qquad \bar{A}_{011} = -\frac{\mu}{(\mu^2+\alpha)^2(1-\mu)},$$

$$\bar{B}_{010} = 1, \qquad \bar{B}_{110} = \frac{\gamma(\alpha-\mu^2)}{\mu(\mu^2+\alpha)},$$

$$\bar{B}_{020} = \frac{\gamma(\alpha-\mu^2)}{\mu(\mu^2+\alpha)^2(1-\mu)}, \qquad \bar{B}_{011} = \frac{\mu}{\mu^2+\alpha}.$$

We next consider the center manifold. Let

$$X = h(Y, \eta),$$

where

$$h(0,0) = 0, \qquad Dh(0,0) = 0.$$

Assume that

$$h(Y,\eta) = c_{20}Y^2 + c_{11}Y\eta + c_{02}\eta^2 + o(\rho_4^2),$$

where $\rho_4 = \sqrt{Y^2 + \eta^2}$. Applying the center manifold invariance equation

$$h(Y_{n+1}, \eta_{n+1}) = X_{n+1},$$

and comparing the coefficients of the second-order terms, we obtain

$$c_{20} = \frac{\alpha\gamma + \alpha\mu^2 - \gamma\mu^2 + 3\mu^4 - 2\mu^3}{\mu^2(\mu^2+\alpha)^3(1-\mu)^3}, \qquad c_{11} = \frac{1}{(\mu^2+\alpha)^2(1-\mu)^2}, \qquad c_{02} = 0.$$

Hence, the center manifold is given by

$$X = h(Y,\eta) = \frac{\alpha\gamma + \alpha\mu^2 - \gamma\mu^2 + 3\mu^4 - 2\mu^3}{\mu^2(\mu^2+\alpha)^3(1-\mu)^3}Y^2 + \frac{1}{(\mu^2+\alpha)^2(1-\mu)^2}Y\eta + o(\rho_4^2). \tag{24}$$

After restricting system (23) to the center manifold, we obtain the following reduced equation:

$$Y_{n+1} = g(Y_n, \eta_n),$$

where

$$g(Y,\eta) = Y + \frac{\mu}{\mu^2+\alpha}Y\eta + \frac{\gamma(\alpha-\mu^2)}{\mu(\mu^2+\alpha)^2(1-\mu)}Y^2 + o(\rho_4^2). \tag{25}$$

It follows from (25) that

$$g(0,0) = 0, \qquad g_Y(0,0) = 1, \qquad g_\eta(0,0) = 0, \qquad g_{Y\eta}(0,0) = \frac{\mu}{\mu^2+\alpha} \neq 0.$$

In addition,

$$g_{YY}(0,0) = \frac{2\gamma(\alpha-\mu^2)}{\mu(\mu^2+\alpha)^2(1-\mu)}.$$

In view of

$$\gamma > 0, \qquad 0 < \mu < 1, \qquad \mu^2 + \alpha > 0,$$

we have

$$g_{YY}(0,0) \neq 0$$

if and only if

$$\alpha \neq \mu^2.$$

Consequently, if $\alpha \neq \mu^2$, then all the conditions for a transcritical bifurcation are satisfied. It follows that system (6) undergoes a transcritical bifurcation at $E_2 = (\mu, 0)$ when $\beta = \beta_2$. This proves Theorem 4. $\square$

Proof of Theorem 5. At $\beta = \beta_0 = 2\gamma\sqrt{\alpha}$, the Jacobian matrix of system (6) at E^* has the eigenvalues

$$\lambda_1 = 1 + 2\sqrt{\alpha} + 2\mu\sqrt{\alpha} - \mu - 3\alpha, \qquad \lambda_2 = 1.$$

Since $\mu < \sqrt{\alpha} < 1$, one has $\lambda_1 > 0$. Moreover,

$$\lambda_1 = 1 \quad \Longleftrightarrow \quad \alpha = \left(\frac{1 + \mu + \sqrt{\mu^2 - \mu + 1}}{3} \right)^2.$$

Thus, under the assumptions of the theorem, $|\lambda_1| \neq 1$.

Let

$$x_n = u_n - \sqrt{\alpha}, \qquad y_n = v_n - 2\alpha(1 - \sqrt{\alpha})(\sqrt{\alpha} - \mu),$$

and introduce

$$\eta_n^* = \beta - \beta_0, \qquad \eta_{n+1}^* = \eta_n^*.$$

Then, the critical fixed point is transformed to $(0,0,0)$. Expanding the extended system at $(0,0,0)$, we obtain

$$\begin{cases} x_{n+1} = a_{100}x_n + a_{010}y_n + a_{200}x_n^2 + a_{110}x_n y_n + a_{020}y_n^2 + o(\rho_1^2), \\ y_{n+1} = y_n + b_{001}\eta_n^* + b_{200}x_n^2 + b_{011}y_n\eta_n^* + b_{002}(\eta_n^*)^2 + o(\rho_1^2), \\ \eta_{n+1}^* = \eta_n^*, \end{cases} \tag{26}$$

where

$$\rho_1 = \sqrt{x_n^2 + y_n^2 + (\eta_n^*)^2},$$

and

$$a_{100} = 1 + 2\sqrt{\alpha} + 2\mu\sqrt{\alpha} - \mu - 3\alpha, \qquad a_{010} = -\frac{1}{2\sqrt{\alpha}},$$

$$a_{110} = -\frac{a_{100} - 1}{2\alpha}, \qquad a_{020} = \frac{1}{8\alpha^{3/2}},$$

$$a_{200} = \frac{a_{100}^2 - 1 - \mu\sqrt{\alpha} + \mu - \alpha - \sqrt{\alpha}}{2\sqrt{\alpha}},$$

and

$$b_{001} = \sqrt{\alpha}(1 - \sqrt{\alpha})(\sqrt{\alpha} - \mu),$$

$$b_{200} = -\gamma(1 - \sqrt{\alpha})(\sqrt{\alpha} - \mu), \qquad b_{011} = \frac{1}{2\sqrt{\alpha}},$$

$$b_{002} = \frac{(1 - \sqrt{\alpha})(\sqrt{\alpha} - \mu)}{4}.$$

The linear part of system (26) has the eigenvalues

$$a_{100}, \qquad 1, \qquad 1.$$

An eigenvector corresponding to a_{100} is $(1,0,0)^T$, while an eigenvector and a generalized eigenvector associated with 1 can be chosen as

$$\left(\frac{1}{2\sqrt{\alpha}(a_{100}-1)},1,0\right)^T, \qquad \left(\frac{(1-\sqrt{\alpha})(\sqrt{\alpha}-\mu)}{2(a_{100}-1)^2},0,1\right)^T,$$

respectively. Thus, take

$$\begin{pmatrix} x_n \\ y_n \\ \eta_n^* \end{pmatrix} = P\begin{pmatrix} X_n \\ Y_n \\ \eta_n \end{pmatrix}, \qquad P = \begin{pmatrix} 1 & \frac{1}{2\sqrt{\alpha}(a_{100}-1)} & \frac{(1-\sqrt{\alpha})(\sqrt{\alpha}-\mu)}{2(a_{100}-1)^2} \\ 0 & 1 & 0 \\ 0 & 0 & 1 \end{pmatrix}. \tag{27}$$

For convenience, set

$$q = \frac{1}{2\sqrt{\alpha}(a_{100}-1)}, \qquad z = \frac{(1-\sqrt{\alpha})(\sqrt{\alpha}-\mu)}{2(a_{100}-1)^2}.$$

The center manifold can be written as

$$X = h(Y,\eta), \qquad h(0,0) = 0, \qquad Dh(0,0) = 0.$$

Since

$$X = h(Y,\eta) = O(\rho_2^2), \qquad \rho_2 = \sqrt{Y^2+\eta^2},$$

it follows from the transformation (27) that

$$x = qY + z\eta + O(\rho_2^2).$$

Therefore,

$$x^2 = q^2Y^2 + 2qzY\eta + z^2\eta^2 + o(\rho_2^2).$$

Restricting the transformed system to the center manifold gives

$$Y_{n+1} = g(Y_n,\eta_n),$$

where

$$\begin{aligned} g(Y,\eta) = {} & Y + b_{001}\eta + b_{200}q^2Y^2 \\ & + (b_{011} + 2b_{200}qz)Y\eta + (b_{002} + b_{200}z^2)\eta^2 + o(\rho_2^2). \end{aligned} \tag{28}$$

Hence,

$$g(0,0) = 0, \qquad g_Y(0,0) = 1,$$
$$g_\eta(0,0) = \sqrt{\alpha}(1-\sqrt{\alpha})(\sqrt{\alpha}-\mu) \neq 0,$$

and

$$g_{YY}(0,0) = -\frac{\gamma(1-\sqrt{\alpha})(\sqrt{\alpha}-\mu)}{2\alpha(a_{100}-1)^2} \neq 0.$$

The retained $Y\eta$ and η^2 terms do not alter these two nondegeneracy quantities. Therefore, all conditions for a saddle-node bifurcation are satisfied. Hence, system (6) undergoes a saddle-node bifurcation at E^* when $\beta = \beta_0$. This proves Theorem 5. □

4. Numerical Simulations

Consistent with the unit-step formulation specified in Section 1, all computations were performed with $h = 1$ in MATLAB R2024b, without using an external continuation or bifurcation package. The equilibrium branches were generated directly from the analytical fixed-point formulas. At every sampled branch point, stability was assigned from the moduli of the two eigenvalues of the Jacobian matrix, using a numerical tolerance of 10^{-8}. Sink, saddle, and source branches are represented by blue solid, orange dashed, and red dash-dotted curves, respectively.

For every representative orbit in the phase portraits, 2000 iterations were computed, and the complete orbit was displayed; no transient iterates were discarded. The arrows indicate the forward iteration direction.

These trajectories are numerical illustrations for the explicitly reported parameter ranges and initial conditions only. They do not constitute a proof of boundedness, dissipativity, uniform persistence, or a complete basin-of-attraction analysis, and no conclusions about arbitrary non-negative initial data are drawn from them.

For the transcritical bifurcation at $E_1 = (1, 0)$, take $\mu = 0.30$, $\alpha = 1.20$, and $\gamma = 0.50$. Then, $\beta_1 = \gamma(1 + \alpha) = 1.10$. The boundary branch was sampled at 2101 values on $1.02 \leq \beta \leq 1.23$ ($\Delta\beta = 10^{-4}$), and the positive branch E_3 was sampled at 1600 parameter values on $1.1000001 \leq \beta \leq 1.23$. Figure 1 shows the equilibrium branches, pointwise stability, and multiplier moduli. At $\beta = 1.14$, $E_3 = (0.824405, 0.173083)$ is a sink, in agreement with the Jacobian multipliers.

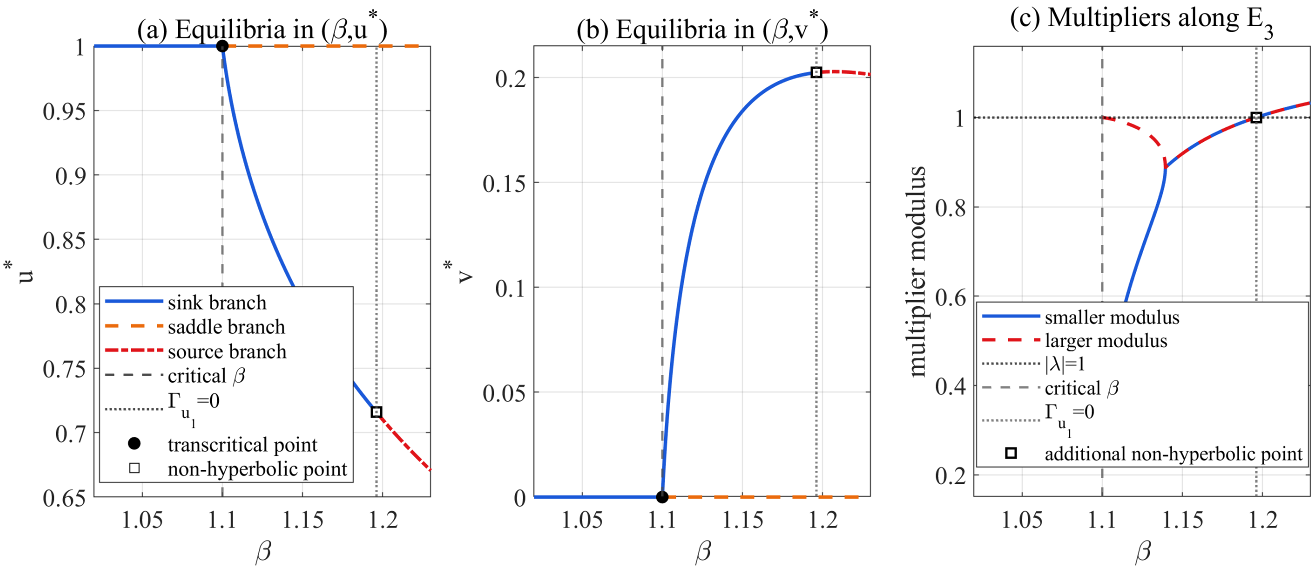

Figure 1. Equilibrium branches and multiplier moduli associated with the transcritical bifurcation at E_1. Colors and line styles identify stability as shown in the legends. The gray dashed and dotted vertical lines mark $\beta = \beta_1$ and $\Gamma_{u_1} = 0$, respectively; the horizontal dotted line in panel (**c**) marks $|\lambda| = 1$. Filled circles mark the transcritical point, and the open squares in all panels mark the same additional non-hyperbolic point at $\beta \approx 1.19602046$. Overlapping segments have identical coordinates.

The corresponding phase portraits are shown in Figure 2.

For the transcritical bifurcation at $E_2 = (\mu, 0)$, take $\mu = 0.50$, $\alpha = 0.10$, and $\gamma = 0.50$. The critical value is $\beta_2 = 0.35$. The boundary branch was sampled at 1701 values on $0.28 \leq \beta \leq 0.45$ ($\Delta\beta = 10^{-4}$), while the positive branch E_4 was sampled at 1400 parameter values on $0.3500001 \leq \beta \leq 0.45$. Stability was again computed independently at every branch point. The corresponding equilibrium branches and phase portraits are shown in Figures 3 and 4, respectively.

https://doi.org/10.3390/math14173198

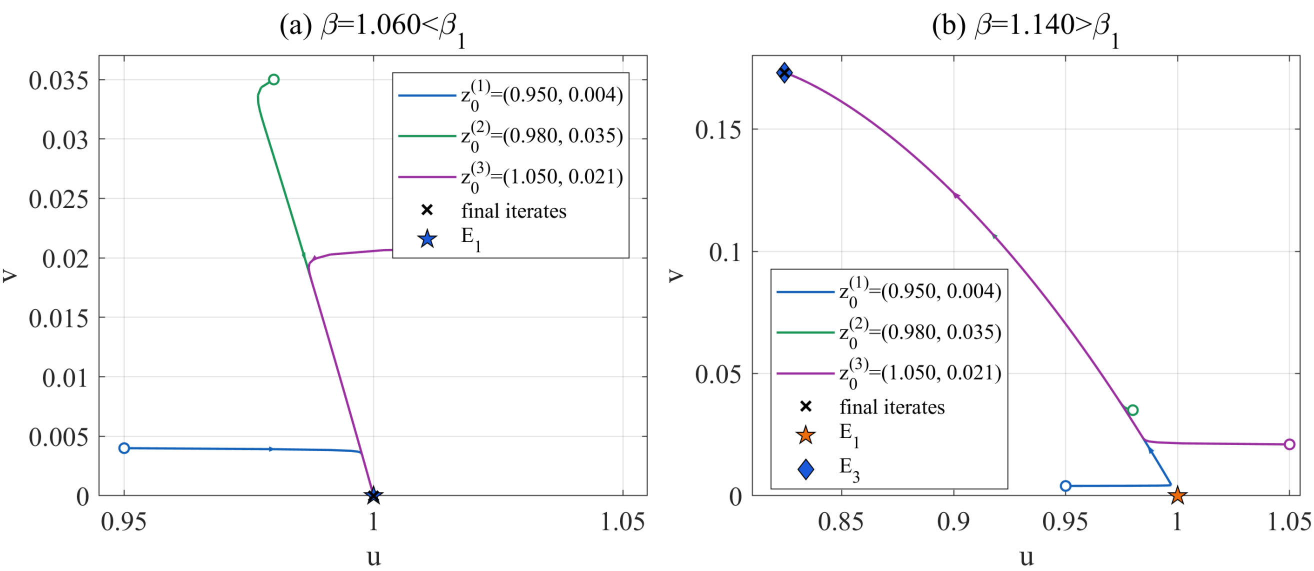

Figure 2. Phase portraits associated with the transcritical bifurcation at E_1 for $\beta = 1.06 < \beta_1$ and $\beta = 1.14 > \beta_1$. The three initial conditions in both panels are $(0.950, 0.004)$, $(0.980, 0.035)$, and $(1.050, 0.021)$. Each complete orbit contains 2000 iterates; open circles, arrows, and crosses mark the initial states, forward direction, and final iterates, respectively. The star and diamond mark E_1 and E_3; overlapping segments share the same forward path.

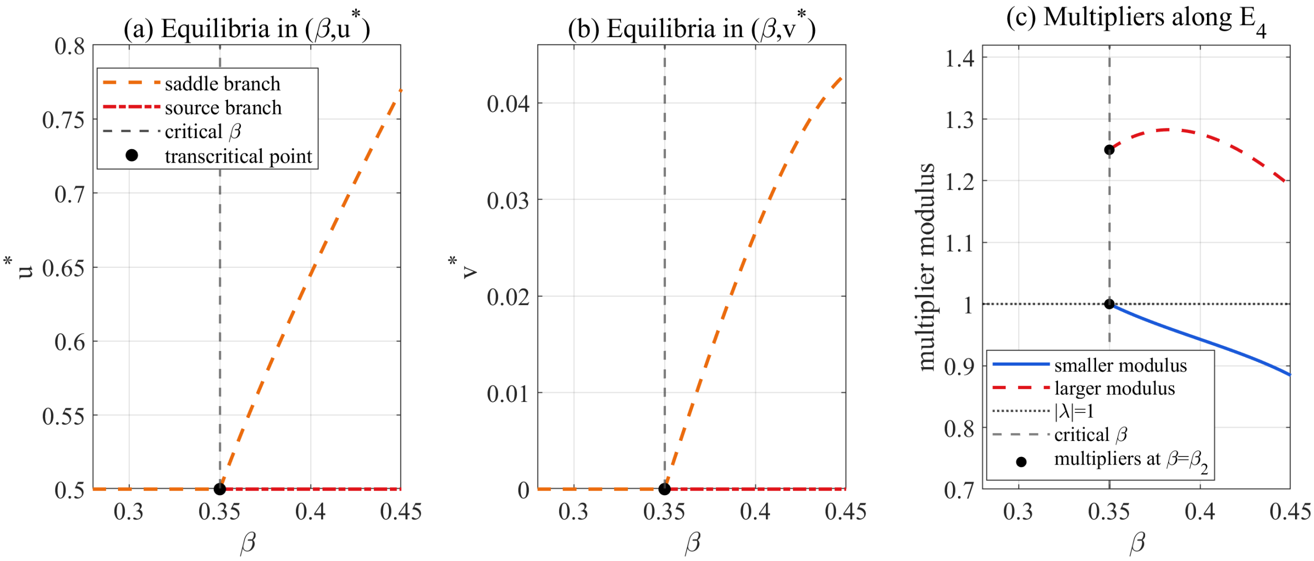

Figure 3. Equilibrium branches and multiplier moduli associated with the transcritical bifurcation at E_2. Colors and line styles are identified in the legends; coincident segments have identical coordinates. The filled circles in panel (**c**) mark both multiplier moduli at $\beta_2 = 0.35$, one of which equals one; no further unit-modulus crossing occurs on the displayed E_4 branch.

For the saddle-node bifurcation at E^*, take $\mu = 0.30$, $\alpha = 0.75$, and $\gamma = 0.50$. These values satisfy the assumptions of Theorem 5. The critical parameter and fixed point are

$$\beta_0 = 2\gamma\sqrt{\alpha} = 0.8660254038, \qquad E^* = (0.8660254038, 0.1137495374).$$

The two positive branches were each sampled at 1600 parameter values on $\beta_0 + 10^{-8} \leq \beta \leq 0.8745$. The lower branch E_3 is a sink, and the upper branch E_4 is a saddle in the displayed neighborhood. The equilibrium branches and phase portraits are shown in Figures 5 and 6, respectively.

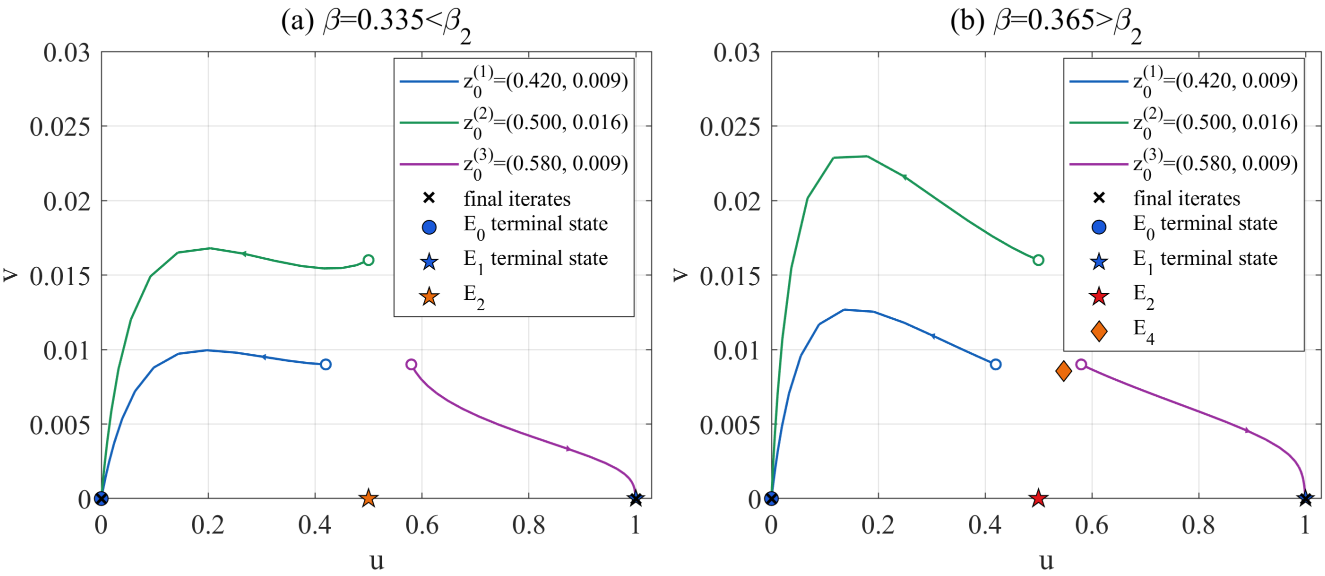

Figure 4. Phase portraits associated with the transcritical bifurcation at E_2 for $\beta = 0.335 < \beta_2$ and $\beta = 0.365 > \beta_2$. The three initial conditions in both panels are $(0.420, 0.009)$, $(0.500, 0.016)$, and $(0.580, 0.009)$. Each complete orbit contains 2000 iterates; open circles, arrows, and crosses mark the initial states, forward direction, and final iterates. The terminal boundary states E_0 and E_1 are included; coincident endpoint and equilibrium markers indicate convergence.

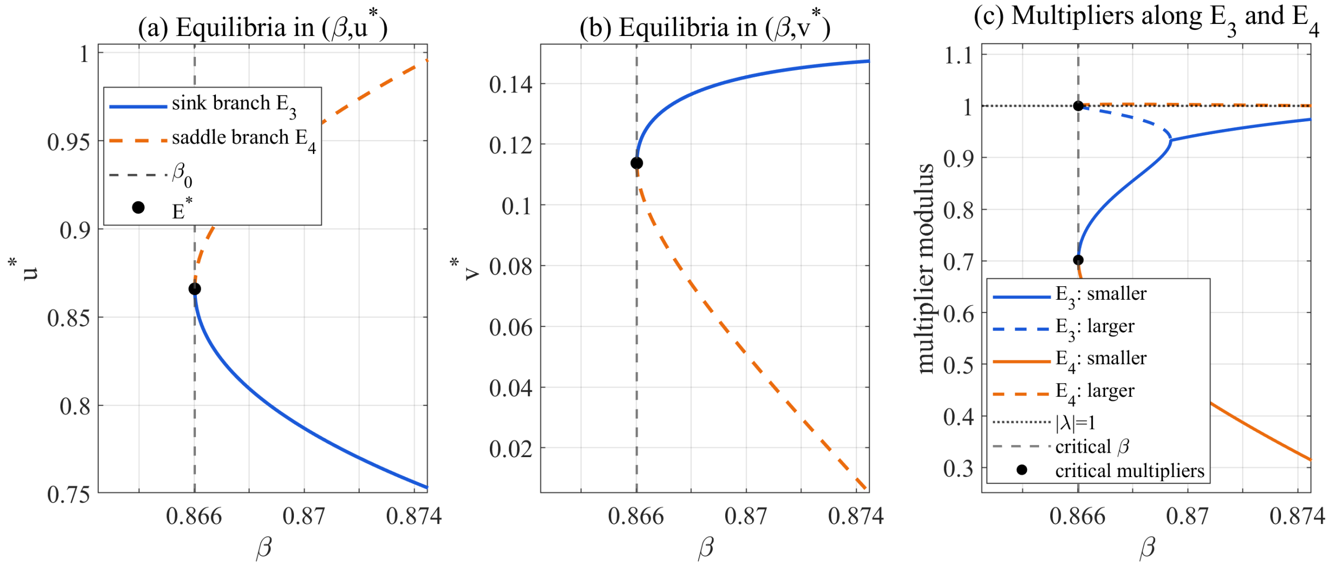

Figure 5. Saddle-node equilibrium branches and multiplier moduli at E^* for $\beta_0 = 0.8660254038$. The blue E_3 and orange E_4 curves meet at E^*; this overlap is the saddle-node collision. The filled points in panel (**c**) mark both multiplier moduli at the collision, one of which equals one.

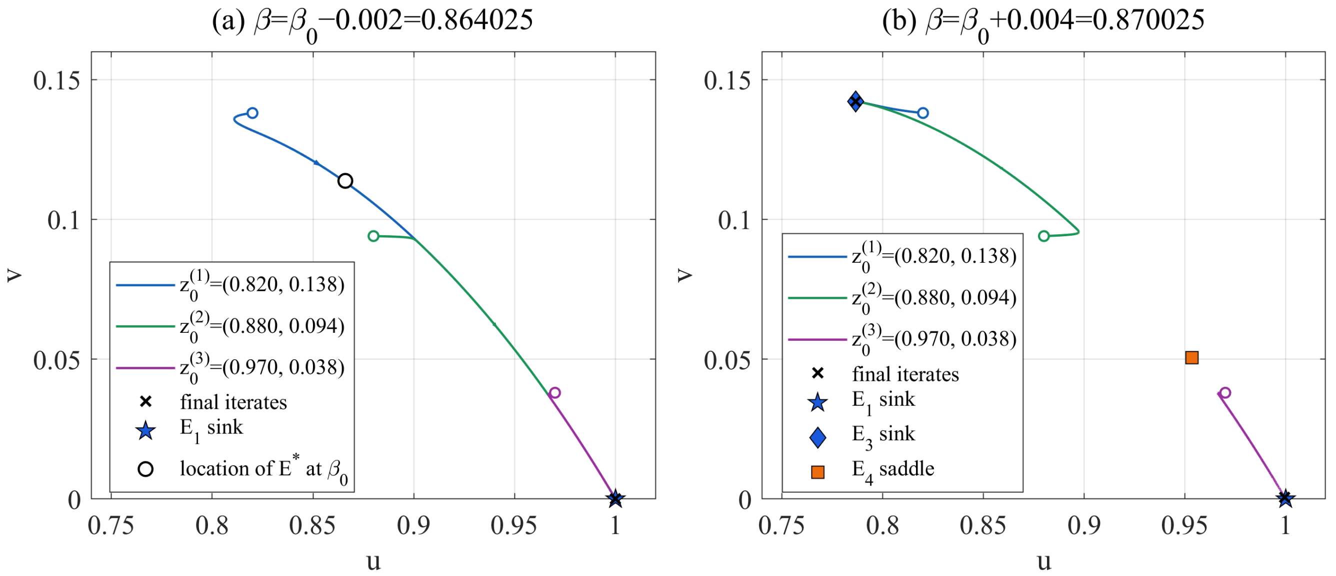

Figure 6. Phase portraits before and after the saddle-node bifurcation at E^*, with $\beta = \beta_0 - 0.002$ and $\beta = \beta_0 + 0.004$. The three initial conditions in both panels are $(0.820, 0.138)$, $(0.880, 0.094)$, and $(0.970, 0.038)$. Each complete orbit contains 2000 iterates; open circles, arrows, and crosses mark the initial states, forward direction, and final iterates. The remaining symbols identify the equilibria shown in the legends.

5. Conclusions

In this paper, a discrete predator–prey system with an Allee effect and a Holling-IV functional response is investigated. By applying the semi-discretization method, the corresponding discrete model is derived from the continuous system. Under assumptions $0 < \mu < 1$, $\alpha > 0$, $\beta > 0$, and $\gamma > 0$, the existence of non-negative fixed points is discussed in detail. In particular, the positive fixed points are characterized by the roots of an auxiliary equation, and their number and distribution are classified according to the relative positions of μ, $\sqrt{\alpha}$, and 1.

Furthermore, the local stability of the boundary fixed points and positive fixed points is analyzed using the eigenvalues of the Jacobian matrix together with the stability criteria for two-dimensional discrete systems. The results show that the boundary fixed point $E_1 = (1, 0)$ changes from a sink to a saddle as β passes through the critical value β_1, while the boundary fixed point $E_2 = (\mu, 0)$ changes from a saddle to a source as β passes through the critical value β_2. For positive fixed points, different stability conditions are obtained according to whether the fixed point lies on the left branch, the right branch, or the critical position $u = \sqrt{\alpha}$.

Finally, using the center manifold theorem and local bifurcation theory, we establish transcritical bifurcations at E_1 when $\beta = \beta_1$ and at E_2 when $\beta = \beta_2$, together with a saddle-node bifurcation at E^* when $\beta = \beta_0$ under the assumptions of Theorem 5. The numerical simulations illustrate the corresponding local equilibrium branches and stability changes. All conclusions obtained here are local and do not establish global predator persistence, stable coexistence, or ecological transitions for arbitrary initial conditions. From a conservation perspective, the Allee and bifurcation thresholds may serve as qualitative warning indicators for low-density prey recovery, predator invasion, and the possible loss of coexistence states. Nevertheless, because these thresholds arise from a local analysis, they should not be interpreted as global management criteria. The conditions $\Gamma_{u_1} = 0$ at E_3 and $\gamma = \delta$ at E_4 only identify possible Neimark–Sacker and flip bifurcations, respectively. Their rigorous study can likewise employ center-manifold and normal-form methods but requires substantially more involved transversality, nonresonance, and higher-order nondegeneracy calculations; it is therefore omitted here. These two positive-equilibrium bifurcations, global boundedness and basin analysis, and the influence of a general step size h are left for future work.

Author Contributions: Conceptualization, J.C.; methodology, J.C. and X.L.; software, J.C.; validation, X.L.; formal analysis, J.C. and X.L.; investigation, X.L.; resources, X.L.; data curation, X.L.; writing—original draft, J.C.; writing—review and editing, X.L.; visualization, X.L.; supervision, X.L.; project administration, X.L.; funding acquisition, X.L. All authors have read and agreed to the published version of the manuscript.

Funding: This work is partly supported by the National Natural Science Foundation of China (61473340), the Distinguished Professor Foundation of Qianjiang Scholar in Zhejiang Province (F708108P01), and the Natural Science Foundation of Zhejiang University of Science and Technology (0401108P10).

Data Availability Statement: The original contributions presented in this study are included in the article. Further inquiries can be directed to the corresponding author.

Acknowledgments: The authors thank the editor-in-chief and the reviewers for their constructive comments. The financial support of this work is also gratefully acknowledged. The authors declare that artificial intelligence (AI) tools were used for language polishing and editing assistance during the preparation of this article. The authors have reviewed and revised the content and take full responsibility for the final manuscript.

Conflicts of Interest: The authors declare no conflicts of interest.

References

1. Rosenzweig, M.L.; MacArthur, R.H. Graphical representation and stability conditions of predator–prey interactions. *Amer. Natur.* **1963**, *97*, 209–223. [CrossRef] [PubMed]
2. Sen, M.; Banerjee, M.; Morozov, A. Bifurcation analysis of a ratio-dependent prey–predator model with the Allee effect. *Ecol. Complex.* **2012**, *11*, 12–27. [CrossRef]
3. Ye, Y.; Liu, H.; Wei, Y.; Zhang, K.; Ma, M.; Ye, J. Dynamic study of a predator–prey model with Allee effect and Holling type-I functional response. *Adv. Differ. Equ.* **2019**, *2019*, 369. [CrossRef]
4. Arsie, A.; Kottegoda, C.; Shan, C. High codimension bifurcations of a predator–prey system with generalized Holling type III functional response and Allee effects. *J. Dynam. Differ. Equ.* **2023**, *35*, 3355–3380. [CrossRef]
5. Zeng, Y.; Yu, P. Multistable states in a predator–prey model with generalized Holling type III functional response and a strong Allee effect. *Commun. Nonlinear Sci. Numer. Simul.* **2024**, *131*, 107846. [CrossRef]
6. Seo, G.; Kot, M. A comparison of two predator–prey models with Hollings type I functional response. *Math. Biosci.* **2008**, *212*, 161–179. [CrossRef] [PubMed]
7. Hsu, S.-B.; Hwang, T.-W. Hopf bifurcation analysis for a predator–prey system of Holling and Leslie type. *Taiwan. J. Math.* **1999**, *3*, 35–53. [CrossRef]
8. Wang, L.-L.; Fan, Y.-H.; Li, W.-T. Multiple bifurcations in a predator–prey system with monotonic functional response. *Appl. Math. Comput.* **2006**, *172*, 1103–1120. [CrossRef]
9. AL-Kaff, M.O.; El-Metwally, H.A.; Elabbasy, E.-M.M. Qualitative analysis and phase of chaos control of the predator–prey model with Holling type-III. *Sci. Rep.* **2022**, *12*, 20111. [CrossRef] [PubMed]
10. Shang, Z.; Qiao, Y. Bifurcation analysis of a Leslie-type predator–prey system with simplified Holling type IV functional response and strong Allee effect on prey. *Nonlinear Anal. Real. World Appl.* **2022**, *64*, 103453. [CrossRef]
11. Lv, L.; Li, X. Stability and bifurcation analysis in a discrete predator–prey system of Leslie type with ratio-dependent simplified Holling type IV functional response. *Mathematics* **2024**, *12*, 1803. [CrossRef]
12. Hu, Z.; Teng, Z.; Zhang, L. Stability and bifurcation analysis of a discrete predator–prey model with non-monotonic functional response. *Nonlinear Anal. Real. World Appl.* **2011**, *12*, 2356–2377. [CrossRef]
13. Huang, J.; Liu, S.; Ruan, S.; Xiao, D. Bifurcations in a discrete predator–prey model with nonmonotonic functional response. *J. Math. Anal. Appl.* **2018**, *464*, 201–230. [CrossRef]
14. Yao, W.; Li, X. Bifurcation difference induced by different discrete methods in a discrete predator–prey model. *J. Nonlinear Model. Anal.* **2022**, *4*, 64–79.
15. Carr, J. *Applications of Centre Manifold Theory*; Springer: New York, NY, USA, 1981.

16. Guckenheimer, J.; Holmes, P. *Nonlinear Oscillations, Dynamical Systems, and Bifurcations of Vector Fields*; Springer: New York, NY, USA, 1983.
17. Kuznetsov, Y.A. *Elements of Applied Bifurcation Theory*, 4th ed.; Springer: Cham, Switzerland, 2023.
18. Wiggins, S. *Introduction to Applied Nonlinear Dynamical Systems and Chaos*, 2nd ed.; Springer: New York, NY, USA, 2003.